Master Thesis in Physics

Quantum Simulators with carbon nanotubes

Submitted by: **Julia Niwemuto**

-May 2024-

This master's thesis is submitted to the East African Institute for Fundamental Research for partial fulfillment of the requirement of the Master's Degrees

Supervisor: Prof. Anna Sanpera Trigueros
Grup d'Informació Quàntica, Univ. Autònoma de Barcelona, Spain

Acknowledgements

I start off by expressing my deepest gratitude to my supervisor, Professor Anna Sanpera Trigueros for her invaluable support and guidance in the duration of this master's thesis. Her expertise and encouragement have been pivotal in shaping my research journey and academic growth.

I would like to thank The World Academy of Science - TWAS for supporting me financially throughout the master's program. This support has allowed me to achieve my academic goals and has been crucial in the completion of this thesis. I am grateful to my professors and instructors who equipped me with knowledge and imparted me with their passion for physics. I am equally grateful to my colleagues and the PhD researchers at the ICTP-EAIFR whose insights and discussions have been of great use in the completion of this master's thesis.

I would like to also acknowledge the contributions of Dr. Utso Bhattacharya, Dr. Lin Zhang, Dr. Stefan Frostner from the ICFO, and in particular Mr. David Ulrich from UAB for their help and joint calculations in this master's thesis. Their expertise and insights were of utmost significance to this work.

Finally, I thank my family and friends for their encouragement, support, and understanding throughout this journey. Their love, patience, and belief in me have been my greatest source of strength and motivation.

This thesis would not have been possible without the collective efforts and support of all those mentioned above. I am truly grateful for their contributions and I am honored to have had the opportunity to work with such dedicated individuals.

ABSTRACT

Quantum electro-nanomechanics devices are becoming increasingly used as ultraprecise tools for quantum phenomena at the mesoscopic scale. Their potential applications are broad, ranging from quantum simulators of complex condensed matter physics to the study of new materials, but also showcasing the potential for quantum technologies. In this master thesis, the focus is put on a new platform consisting of carbon nanotubes suspended in leads and manipulated with external electric fields. The system bears similitudes to polaritonic physics, where now phonons are coupled to electrons. My master thesis work has explored in detail such systems. Firstly, understanding and reproducing analytically previous results concerning the interactions arising between different quantum dots suspended in carbon nanotubes. Secondly, we have extended previous analytical results making use of perturbation theory. Finally, we have introduced a novel model with the aim of extending previous one-dimensional studies to two-dimensional quantum simulators. Such a model offers the potential to implement quantum gates and opens the door to extend the use of nano-mechanical devices to quantum computation.

CONTEXT AND MOTIVATION

Presently, one of the most active fields of research in condensed matter physics is the study of strongly correlated quantum systems. Such a vast field of research has enormously benefitted in the last years from quantum simulators that use atoms, ions, Rydberg atoms, molecules, nitrogen-vacancy centers quantum dots, and others to mimic some paradigmatic models of many correlated systems. Those included Bose and Hubbard, Holstein, or Frölich-Coulomb models, where particle-particle interaction leads to important correlation effects with significantly different properties, like the ones arising, for instance, in high-temperature superconductors. Among the strongly correlated systems, I focus here on the electron-phonon class of models, which showcase the interactions between electrons as well as interactions between electrons and phonons. My work is inspired by two previous articles, *Phonon induced pairing in quantum dot quantum simulators*[2] and its posterior extension *Steady-state Peierls transition in nanotube quantum simulator* by the same group [7]. Our study, however, incorporates independent nano-tubes and opens a new phase diagram that has, as a limit, the previous ones.

The motivation of this master thesis lies in advancing the understanding of strongly correlated systems while proposing novel architectures to exploit the exquisite precision achieved by such systems. As a final goal, there is an interest in exploring those novel platforms and investigating their potential for two-dimensional quantum simulators and their applications for quantum computing.

PROJECT DESCRIPTION

The structure of this Master's thesis is as follows: In Section 1, I introduce the basic concepts concerning carbon nanotubes, quantum dots, and how quantum dots in carbon nanotubes are created in the lab. We also use this section to introduce the paradigmatic models of strongly correlated systems, namely Bose-Hubbard and Fermi-Hubbard Hamiltonians due to the close analogy with the model presented. Section 2, deals with the theoretical background needed to describe such systems. There, I derive first the full Hamiltonian describing a single suspended carbon nanotube, hosting an arbitrary number of quantum dots on it. Though presently it is difficult to create experimentally more than four quantum dots in present carbon nanotubes, it is interesting to analyze the results for different numbers of quantum dots. To get some analytical insight into the physics of the problem, it is necessary to reduce its complexity. To this aim, I use a unitary

transformation known as the Lang-Firsov approximation, widely used in condensed matter physics to describe polarons. It will be fundamental to attack the problem analytically and to derive an approximate phase diagram of the system. In Section 3, I analyze in detail the different phases and phenomena arising in a single carbon nanotube and derive the corresponding phase diagram of the model for different initial conditions. To this aim we first use atomic limit, that is, when the tunneling of electrons between different carbon nanotubes is neglected. Further, to take into account tunneling, we have developed an oversimplied degenerate perturbation theory which demonstrates how the quantum phase transition of the model changes as tunneling is included. Our model of perturbation theory has, however, some severe limitations and needs to be refined further as we will explain. In Section 4, I report some original contributions to this field. First, we have extended the system of study to two parallel suspended nanotubes with several quantum dots on each and allow interactions between the two carbon nanotubes. This setup provides a much richer, though also much more complex physics. We first derived the new Hamiltonian using the Lang-Firsov transformation and analyzed (in the atomic limit) the corresponding phase diagram. The full phase diagram of this system can only be numerically addressed, but even in the limiting cases I have analyzed, interesting physics appears. Finally, in Section 5, I summarize our more important results and present the concluding remarks together with a list of open questions to be addressed.

Keywords: Quantum simulators, carbon nanotubes, quantum dots, Bose-Holstein models, polaritonic physics.

List of Abbreviations

Abbreviation	Full Name
CNT	Carbon nanotube
QD	Quantum dots
QS	Quantum simulators
BH	Bose Hubbard models
PL	Polaritonic states
EPCM	Electron-Phonon Class of Models
MI	Mott Insulating state
PS	Pair state
QPT	Quantum Phase Transition

Contents

1 Introduction

1.1 Quantum Simulators

Quantum simulators are experimental systems designed to replicate simplified versions of complex systems used in different fields of physics and chemistry, for instance in condensed matter physics. These simulators are particularly valuable as they can tackle problems too computationally demanding for classical computers. Though presently, the main advantage of quantum simulators lies in their ability to address scientific challenges that classical computers struggle to simulate efficiently due to high computational costs, they are expected to be a very valuable tool for example, in material science allowing the exploration and design of materials with novel properties. To ensure the accuracy of these simulations, quantum simulators offer precise control over parameters and states within the simulated system. This control is essential for validating the simulator's results, which can be achieved through various methods. These methods include comparing the simulation's outcomes to results from classical simulations of manageable models or examining the simulated system's behavior against established scientific constraints (see e.g. [4] and references therein).

A paradigmatic example of a quantum simulator consists of ultracold atoms loaded optical lattices. In such systems (as well as in many others), there is the possibility to mimic effective Hubbard-like models with diverse geometries and tunable interactions, that is, Hamiltonians of the form.

$$H_{Hubbard} = -t \sum_i (c_i^\dagger c_j + h.c.) + U \sum_{i,j} n_i n_j \tag{1}$$

where i, j are multi-indices, according to the geometry of the configuration, and the creation and annihilation operators can be bosonic or fermionic. Such class of Hamiltonians comprises as well typical Heisenberg XX, XY, or XYZ models, with variable interactions, disordered systems, dipolar interactions, etc..[4]

1.2 Nano-mechanical quantum devices

Carbon nanotubes (CNT) sustaining quantum dots (QD) could, on the other hand, provide a platform for simulating and probing strongly correlated electron physics interacting with phonons, a type of model that cannot be addressed in optical lattices, where phonons are absent due to the "rigidity" of the optical lattice formed by two counterpropagating lasers of equal frequency. Indeed, one of the most active fields of research in condensed matter physics nowadays is the study of strongly correlated effects in electro-nanomechanical systems.

Among strongly correlated systems, in this master thesis I focus on the so-called *Electron-Phonon Class of Models* (EPCM) [1], which refer to electronic models where asides of the interactions between electrons, a prominent role is played by the coupling between electrons and phonons. Their Hamiltonians are of the type

$$H_{Hubbard} = -t \sum_i (c_i^\dagger c_j + h.c.) + U \sum_{i,j} n_i n_j + \sum_\alpha \omega_\alpha b_\alpha^\dagger b_\alpha + \sum_{i,\alpha} g_{i,\alpha} n_i (b_\alpha + {}_\alpha^\dagger) \tag{2}$$

Our model lies in such a class, but before proceeding further we explain here in some detail the model under consideration: quantum dots in suspended carbon nanotubes (CNT).

1. **Carbon nanotubes** Roughly speaking, carbon atoms allow to create fascinating structures in all dimensions. Carbon-60 is a molecule made of 60 Carbon atoms with a football structure (fullerene) and corresponds to a zero-dimensional model, carbon nanotubes are 1D models, graphene layers are 2D models and graphite is a truly 3D model. In all the above materials, each carbon atom is covalently bonded with three adjacent carbon atoms in a honeycomb lattice, as displayed in Figure (1). Their atomic structures are closely related, and graphene can be viewed as the fundamental building block of 1D, 2D, and 3D structures.

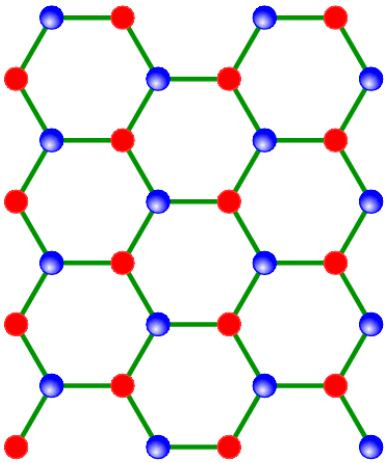

Figure 1: The honeycomb lattice of graphene, displays the (covalent) bonds of each carbon atom with their neighboring carbon atoms.

A carbon nanotube (CNT), see Fig.2, corresponds to a rolled-up monolayer graphene sheet. The CNT has diameters in the nanometer (nm) scale and variable lengths up to some hundreds of nm. CNTs are known to have great strength and stiffness because the binding of carbon to make a cylindrical-shaped structure is more stable than any other structure of carbon. Moreover, they possess very interesting high electrical and thermal conductivity as well as amazing mechanical properties. Different CNT properties need to be considered for different types of quantum device applications. For CNT quantum dots, most of the physics is a consequence of the one-dimensional confinement of electrons occurring on a hexagonal lattice. The chirality in nanotubes is not essential, but what is important is to use narrow-gap nanotubes because their Fermi energy can be tuned easily by electrostatic gating, and this is a property that will be essential for an electro-nanomechanical device. In general, such CNTs have very few defects, making them ideal for applications at the quantum level. Single-walled carbon nanotubes (SWCNTs) have diameters around 0.5–2.0 nm and can be obtained from a two-dimensional graphene sheet rolled up to form a hollow cylinder. There exist also the so-called, Multi-walled carbon nanotubes (MWCNTs), consisting in a nested structure of single-wall carbon nanotubes as displayed in Fig. 2. In our case, we will focus on singled-walled CNT.

2. **Quantum dots** A quantum dot is a nano-scale structure made of semiconducting materials that can trap and confine electrons in a small space. They possess remarkable quantum mechanical properties and unique optical and electronic properties. Due to this reason, they are widely used in electronics and biotechnology, and current research is made around their applications in quantum computing, solar cells, and medical imaging. They can be considered to be artificial atoms because like atoms

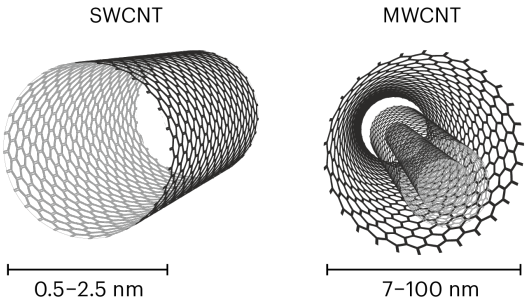

Figure 2: Image of Single- and Multi-Walled Carbon nano-tubes.

they have discrete energy levels due to the confinement of electrons in small space. But unlike atoms, their electronic wavefunctions are widely spread out, and the electron-electron interactions are more complex in quantum dots.

3. **Carbon nanotubes quantum dots**

The synthesis of quantum dots, as referenced in [5], involves first fabricating carbon nanotubes by Chemical Vapor Deposition. The nanotubes are grown directly on chips pre-patterned with electrodes and trenches using a catalyst and chemical vapor deposition (CVD). The catalyst is patterned into rectangular islands on the source/drain electrodes. To minimize unwanted nanotubes that create electrical shorts to the gate electrodes, a SiO2 layer is evaporated onto the chip covered with an electron beam lithography resist used to pattern the catalyst structures. After drop casting the catalyst, the catalyst remains attached to the SiO2 layer during the resist lift-off, reducing nanotubes grown from the catalyst in unwanted regions.

Additionally, the electrical connections between the gate electrodes and the wire-bonding pads are encapsulated with a SiO2 layer to minimize shorts by undesired nanotubes between electrodes.

A CNT quantum dot (CNTQD), or an artificial atom, is formed when a single CNT is suspended between two electrical contacts as indicated in Figure 3.

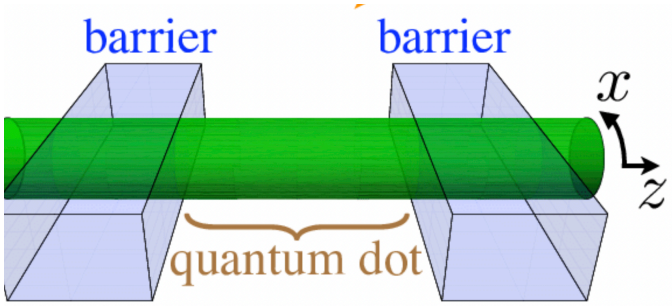

Figure 3: Schematical display of a quantum dot created on a suspended carbon nanotube employing electrostatic potentials forming potential barriers.

In such a situation, electrons are confined in a potential well with discrete energy levels. Electrons can be added to these energy levels one by one. CNT-based QDs have very interesting properties for quantum technological applications. The advantages of using CNTQDs are several. First, one can define spin qubits with two CNTQD that have longer spin relaxation as compared to traditional semiconductor-based

charge qubits, since spin-orbit interaction is very small and there is no nuclear spin interaction in CNTs.

In our work, we focus on a very recent proposal of coupling the flexural modes of a CNT to an integrated quantum dot, with the dot itself defined in the nanotube[6, 2], as shown in the figure here below. Another very important advantage is they can reach a very strong coupling regime between the mechanical models of the nanotube characterized by frequencies ω_n and the coupling of the quantum dot electron to the phononic modes of the CNT, that we denote by g. The ultrastrong regime in an electrical-nanomechanical device is reached when the ratio $\Gamma = g/\omega > 1$. For instance, a QD in a semiconductor nanowire has a coupling of $\Gamma \approx 0.85$, while in a CNTQD $\Gamma \simeq 2.7$ reaching the ultrastrong coupling regime [6].

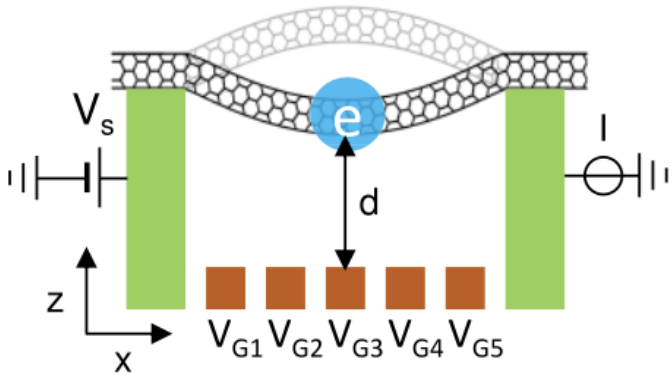

Figure 4: Figure taken from [6] displays the Flexural modes of CNT which hosts a quantum dot.

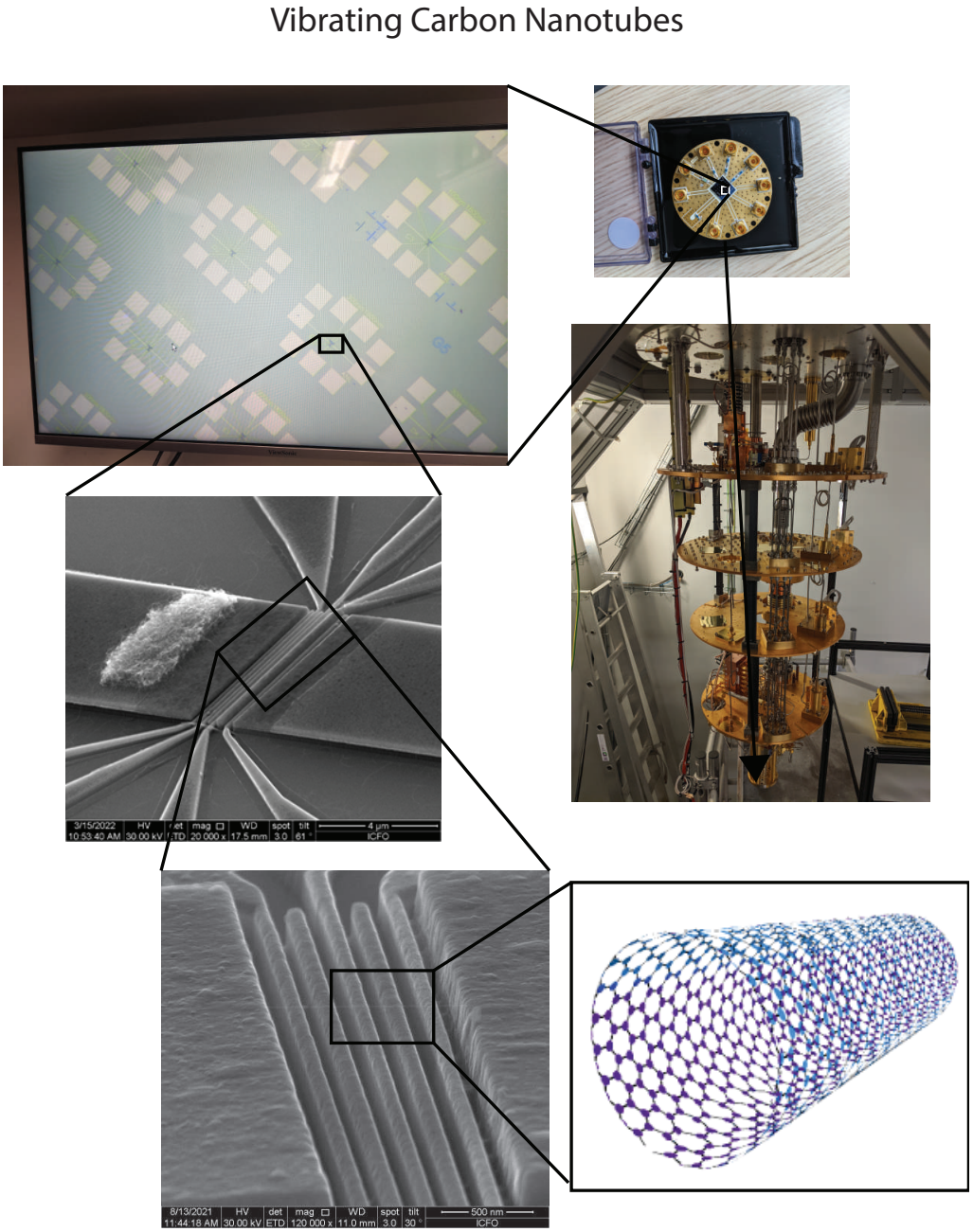

Figure 5: This figure gently provided by ICFO displays the experimental setup used in the Institute of Photonic Sciences (ICFO), for a chip containing several suspended CNT with some QD on them.

In Figure [5] above, the whole shown is the experimental setup of the suspended carbon nanotubes carried out at ICFO. The bottom left is an image from Scanning Electron Microscopy which shows a carbon nanotube suspended over two leads, and five electrode gates beneath the CNT which are used to confine the CNTQD. On its right, a zoomed-out image of a carbon nanotube is displayed. Directly above it, there is another image that zooms on the previous one and shows the creation of the CNTQD together with the five electrode gates and also the image of the source electrode, which is highlighted in gray. The device consists of a carbon nanotube connecting the source and drain electrodes while being suspended over five electrode gates [5]. There are copies of this setup which are

replicated on a chip as is shown in the image at the top of the Figure. The right image on the top shows what the integrated chip looks like and the machine in which this chip is introduced to carry on the experiments (Courtesy of ICFO).

2 System under investigation: Electron-Phonon model

The pursuit of quantum simulations holds promise for unraveling the complexities of strongly correlated electronic systems, which remain challenging for analytical and numerical methods. The paper entitled *Phonon-induced pairing in quantum dot quantum simulator* [2], proposes an experimentally viable approach using a suspended CNT with four embedded QD on it, with one electron populating each, see Fig 6. In this setup, the CNTQD replicates models involving electron-electron and electron-phonon interactions, such as the Hubbard-Holstein model. The system's Hamiltonian features tunable parameters like electron hopping between dots, on-site Coulomb repulsion, and coupling of electrons to the nanotube vibrations or flexural modes which are phonons. Notably, those studies predict the emergence of three distinct phases characterized by a Mott insulating state (MI) dominated by electron-electron interactions at weak electron-phonon coupling, a polaronic paired state with broken symmetry arising from strong electron-phonon coupling, and a delocalized state exhibiting electron pairing correlations and correlated phonon behavior at large hopping. A key finding is the possibility of driving sharp transitions between the Mott and polaronic regimes by tuning the electron-phonon interaction strength, with signatures accessible in local measurements of quantum dot occupancies, even at finite temperatures.

The proposed setup constitutes a highly tunable and theoretically tractable quantum simulator that provides novel insights into strongly correlated physics. Its rich phase diagram, arising from the intricate competition between electron-electron repulsion, electron-phonon attraction, and hopping terms, renders it an interesting setup for exploring electron-phonon models relevant to understanding exotic phenomena like high-temperature superconductivity. The work exemplifies how designer quantum devices can open new frontiers in quantum many-body physics.

In this setup, the four quantum dots act as tunable artificial atoms embedded in a suspended carbon nanotube. The electrons can hop between the dots, experience on-site Coulomb repulsion, and couple to the vibrating modes (phonons) of the nanotube itself, and these parameters like electron hopping, Coulomb interaction, and electron-phonon coupling strength are controllable. What makes this proposal so promising is the ability to use quantum dots as highly tunable artificial lattice sites that can be precisely measured. The predicted phase transitions, from a Mott insulator to a polaronic paired state to a novel delocalized state with phonon correlations, could therefore be detected by monitoring changes in the individual dot occupancies using existing charge sensing techniques. Notice also that the interplay between electrons and phonons and electron-electron repulsion plays a fundamental role in unconventional superconductors.

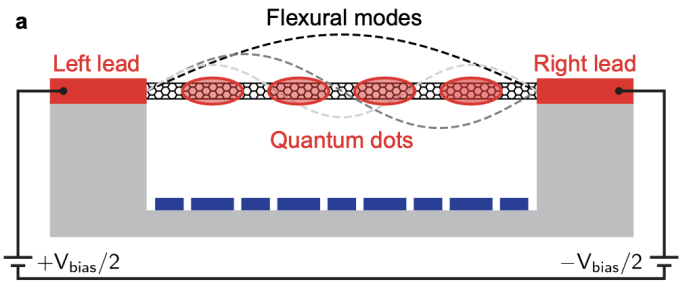

Figure 6: A suspended CNT hosting four quantum dots on it. (From [5])

2.1 Derivation of the system Hamiltonian

The system under investigation is schematically depicted in Figure (6), The most general setup consists of one single CNT suspended in its corresponding leads. On the graphene nanotube, there are several QD, which can host up to some number of electrons. The QD is defined electrostatically along the nanotube with voltages on the gate electrodes specially designed below the nanotube as shown in Fig. (3). We will assume that each quantum dot can be associated with a "potential well", in which electrons can jump. Filled quantum dots located within the same nanotube interact via Coulomb potential. Importantly, there is also *flexural modes* of the nanotube which can be understood as phonons (collective excitations) and play a fundamental role in the physics we are interested in. As it will become clear here, as a result, the quantum dots (electrons) in the nanotubes, can also interact phonon-mediated. Such phonon-mediated electron-electron interactions can be attractive and stabilize the system.

In this master thesis, I have first analyzed the different phases and phenomena arising in a single CNT, and derived in detail the phase diagram of the model for different numbers of initial electrons and QD. I have also extended the configuration displayed in Fig. **??** to the case of two interacting nanotubes, which I will develop in Section 3.

The Hamiltonian corresponding to a single nanotube, with an arbitrary number of QD on it, consists of three terms, describing the electrons, phonons, and the electron-phonon interactions respectively. namely H_e, H_p, and H_{ep}. Explicitly, the most general Hamiltonian for the system, $\hat{H}$, takes the following form:

$$\begin{aligned}\hat{H} &= \hat{H}_e + \hat{H}_p + \hat{H}_{ep} = -t\sum_{i,\sigma}(\hat{c}^\dagger_{i,\sigma}\hat{c}_{i+1,\sigma} + h.c.) + \frac{U}{2}\sum_i(\hat{n}_i(\hat{n}_i - 1)) + \\ &+ \sum_{i\neq j} V\hat{n}_i, \hat{n}_j + \sum_i \mu\hat{n}_i + \sum_\alpha \omega_\alpha \hat{b}^\dagger_\alpha \hat{b}_\alpha + \sum_{i,\alpha} g_\alpha \hat{n}_{i,\alpha}(\hat{b}^\dagger_\alpha + \hat{b}_\alpha). \qquad (3)\end{aligned}$$

The first term of the above Hamiltonian accounts for the possibility that electrons hop from one quantum dot to another. The creation and annhilation electron operators are denoted by $\{\hat{c}^\dagger_{i,\sigma}, \hat{c}_{i,\sigma}\}$, which fulfill fermionic commutation relations $\{\hat{c}_i, \hat{c}_j\} = \delta_{ij}$, where i denotes the quantum dot site in the carbon nanotube. The occupation number on-site i is denoted by $\hat{n}_i = \sum_\sigma \hat{n}_{i,\sigma} = \sum_\sigma c^\dagger_{i,\sigma}\hat{c}_{i,\sigma}$, where σ, σ' account for the spin degree of freedom (polarization: up or down respectively) of the electron. The second term, $\frac{U}{2}\sum_i(\hat{n}_i(\hat{n}_i - 1)$ refers to the local Coulomb repulsion U, which is considered to be the same in each dot. The polarization degree of freedom will be only relevant on this on-site term, as the Pauli exclusion principle forbids double occupancy in the same QD if the electrons are polarized.

The third term, $\hat{n}_i, \hat{n}_j$ describes inter-site Coulomb repulsion. Finally, for the electronic part, there is the term $\sum_i \mu \hat{n}_i$, where μ denotes the chemical potential. This term is needed in case the number of electrons (entering and leaving the system through the two external leads) is not constant. From now on we will consider that the tunneling amplitude from and to the leads of the first and last QD is negligible, so that the total number of electrons remains fixed and the chemical potential term is just a global shift on the energy that can be neglected. The last two terms of the Hamiltonian incorporate the bosonic modes with creation and annihilation operators $\hat{b}^\dagger_\alpha, \hat{b}_\alpha$. These modes correspond to the "flexural" modes (guitar mode) of the CNT, i.e., a bath of phonons (harmonic oscillators) with number density $\hat{b}^\dagger \hat{b}$ and frequency ω_α. Finally, the last term of the Hamiltonian, $g_\alpha \hat{n}_{i,\alpha}(\hat{b}^\dagger_\alpha + \hat{b}_\alpha)$, describes the coupling between the electrons in the QD and the phononic bath. Its strength is given $g_{\alpha,i}$.

The above Hamiltonian is complex and cannot be solved analytically due to the tunneling term which is not quadratic on the creation and annihilation fermionic operators and the electron-phonon interaction, again not quadratic. Several approximations can be taken into account. First of all, we shall consider that the inter-site Coulomb potential V can be neglected in front of the on-site Coulomb interaction U. Secondly, as already said, we consider the system formed by the carbon nanotube with its corresponding quantum dots, to be a closed system, with a fixed number of electrons, discarding thus the chemical potential term proportional μ. Furthermore, we consider here unpolarized electrons at half filling, allowing thus double occupancy of electrons (pairing) in a single quantum dot. With the above simplifications, the full Hamiltonian of the system reads:

$$\begin{aligned} \hat{H} &= \hat{H}_e + \hat{H}_p + \hat{H}_{ep} = -t \sum_{i,\sigma} (\hat{c}^\dagger_{i,\sigma} \hat{c}_{i+1,\sigma} + h.c.) + \frac{U}{2} \sum_{i,\sigma \neq \sigma'} (\hat{n}_{i,\sigma} \hat{n}_{i\sigma'}) + \\ &+ \sum_\alpha \omega_\alpha \hat{b}^\dagger_\alpha \hat{b}_\alpha + \sum_{i,\alpha} g_\alpha \hat{n}_{i,\alpha} (\hat{b}^\dagger_\alpha + \hat{b}_\alpha). \end{aligned} \tag{4}$$

Despite the simplifications, the analytical solution of this Hamiltonian remains unfeasible, due to the tunneling term and the electron-phonon coupling. However, this last term can be brought to a simpler form via a unitary transformation, the so-called Lang-Firsov transformation, which I will extensively use in this master thesis and is explained in the next section.

2.2 The Lang-Firsov approximation

To gain an insight into the physics of the system, it is useful to eliminate first the electron-phonon interaction, greatly reducing the complexity of the full Hamiltonian given by equation (4). To do so, we use the Lang-Firsov transformation [3], widely applied to the extended Holstein-Hubbard model This transformation results in a basis change to polaron-type quasi-particles, that is, electrons surrounded by clouds of vibrations. It corresponds to a unitary transformation on the Hamiltonian

$$H' = U \; H \; U^\dagger \tag{5}$$

where $U = e^S$ and $U^\dagger = e^{-S}$. Since the transformation must be unitary to preserve the Hermiticity of the Hamiltonian, this demands that the transformation's generator S must be anti-Hermitian, $S^\dagger = -S$, chosen in such a way that it cancels out the linear coupling of the electron-phonon coupling. Such transformation leads to an *effective* Hamiltonian, in which the electron-phonon coupling becomes quadratic in the fermionic operators. In

general, that will mean that $S = \lambda({b_\alpha}^\dagger - b_\alpha)n$, where for easiness of notation I have withdrawn the hat symbol in the operators. In our case, it becomes

$$S = \sum_{i,\alpha} \frac{g_\alpha n_i}{\omega_\alpha}({b_\alpha}^\dagger - b_\alpha) \tag{6}$$

The transformation is obviously done on each term in the Hamiltonian. One should expand the exponentials and make use of the Baker-Campbell-Haussdorf formula.

$$\begin{aligned} H' &= e^S H e^{-S} = (1 + S + \frac{S^2}{2!} + \frac{S^3}{3!} + \cdots)H(1 - S + \frac{S^2}{2!} - \frac{S^3}{3!} + \cdots) \\ &= H + SH - HS + \frac{S^2}{2!}H - SHS + H\frac{S^2}{2!} - \frac{S^3}{3!}H + SH\frac{S^2}{2!} - \frac{S^2}{2!}HS + \frac{S^3}{3!}H + \cdots \end{aligned} \tag{7}$$

It is now trivial to see that the above expression can be compactly rewritten as:

$$H' = H + [S, H] + \frac{1}{2!}[S, [S, H]] + \frac{1}{3!}[S, [S, [S, H]]] + \cdots = \frac{1}{m!}\sum_{m=0}^{\infty}[S, H]_m, \tag{8}$$

where $[S, H]_m = [S, [S, ...[S, H]]]$ indicates that the m-order commutator between S and H. To proceed further, we apply the Lang-Firsov transformation to each of the terms of the Hamiltonian, that is

$$H' = e^S H e^{-S} = e^S\, H_e\, e^{-S} + e^S\, H_p\, e^{-S} + e^S\, H_{ep}\, e^{-S} \tag{9}$$

We start by considering first the electronic part:

$$(H_e)' = H_e + [S, H_e] + \frac{1}{2!}[S, [S, H_e]] + \frac{1}{3!}[S, [S, [S, H_e]]] \tag{10}$$

the first term results in:

$$[S, H_e] = -t\sum_{i,\alpha}\frac{(g_{i,\alpha})}{\omega_\alpha}((b_\alpha)^\dagger - b_\alpha)[n_i, (c_i^\dagger c_{i+1} + c_{i+1}^\dagger c_i)] \tag{11}$$

After solving to third order and developing the respective commutators between $n_i = c^\dagger c$ and the creation and annihilation operators one obtains: ¡

$$[n_i, c_1^\dagger c_2] = c_1^\dagger c_2 \tag{12}$$

$$[n_i, c_2^\dagger c_1] = c_2^\dagger c_1 \tag{13}$$

$$\tag{14}$$

Finally, the commutator of the operator S and the tunneling term of the Hamiltonian reads:

$$[S, H_t] = -t\sum_{i,\alpha}\frac{(g_{i,\alpha})}{\omega_\alpha}((b_\alpha)^\dagger - b_\alpha)(c_i^\dagger c_{i+1} + c_{i+1}^\dagger c_i) \tag{15}$$

Now, proceeding further, up to the second order in the expression 8, we find that:

$$[S, [S, H_t]] = -t\sum_{i,j,\alpha,\beta}\frac{(g_{i,\alpha})}{\omega_\alpha}\frac{(g_{j,\beta})}{\omega_\beta}[ni((b_\alpha)^\dagger - b_\alpha), ((b_\beta)^\dagger - b_\beta^A)(c_i^\dagger c_{i+1} + c_{i+1}^\dagger c_i)] \tag{16}$$

$$[S,[S,H_t]] = -t\sum_{i,\alpha,\beta}\frac{(g_{i,\alpha})}{\omega_\alpha}\frac{(g_{i,\beta})}{\omega_\beta}(c_i^\dagger c_{i+1}+c_{i+1}^\dagger c_i) \tag{17}$$

Finally, by joining all the terms, the electron part Hamiltonian, after the Lang-Firsov transformation becomes:

$$\begin{aligned} H_e' = &-t(c_1^\dagger c_2 + h.c) + Vn_1n_3 - t\sum_{i,\alpha}\frac{(g_{i,\alpha})}{\omega_\alpha}((b_\alpha)^\dagger - b_\alpha)(c_i^\dagger c_{i+1}+c_{i+1}^\dagger c_i) \\ &- t\sum_{i,\alpha,\beta}\frac{(g_{i,\alpha})}{\omega_\alpha}\frac{(g_{i,\beta})}{\omega_\beta}(c_i^\dagger c_{i+1}+c_{i+1}^\dagger c_i) \end{aligned} \tag{18}$$

Next, we derive the phonon part of the Hamiltonian:

$$[S,H_p] = [S,\sum_\alpha \omega_\alpha b_\alpha^\dagger b_\alpha] \tag{19}$$

$$[S,H_p] = \sum_{i,\beta}\sum_\alpha \frac{g_{i,\beta}n_i}{\omega_\beta}\omega_\alpha[(b_\beta^\dagger - b_\beta), b_\alpha^\dagger b_\alpha] \tag{20}$$

$$[S,H_p] = \sum_{i,\beta}\sum_\alpha \frac{g_{i,\beta}n_i}{\omega_\beta}\omega_\alpha[(b_\beta^\dagger b_\alpha^\dagger b_\alpha)] - [b_\beta, b_\alpha^\dagger b_\alpha] \tag{21}$$

For the above commutators to be different from zero we require that α=β (otherwise they cancel). Finally, we develop up the second order the expression 8, obtaining

$$[S,H_p] = -\sum_{i,\alpha} g_{i,\alpha}n_i(b_\alpha^\dagger + b_\alpha) \tag{22}$$

$$[S,[S,H_p]] = -\sum_{i,\alpha} g_{i,\alpha}\sum_{j,\beta} g_{i,\beta}[n_i(b_\alpha^\dagger - b_\alpha), n_j(b_\beta^\dagger + b_\beta)] \tag{23}$$

So that:

$$[S,[S,H_p]] = 2\sum_{i,j,\alpha}\frac{g_{i,\alpha}g_{j,\alpha}}{\omega_\alpha}n_in_j \tag{24}$$

Collecting all the above expressions, the transformed Hamiltonian of the phonon part is:

$$H_p' = \sum_\alpha \omega_\alpha b_\alpha^\dagger b_\alpha - \sum_{i,\alpha} g_{i,\alpha}n_i(b_\alpha^\dagger + b_\alpha) + 2\sum_{i,j,\alpha} g_{i,\alpha}g_{i,\alpha}n_in_j \tag{25}$$

The last term to be transformed corresponds to the electron-phonon interaction. Again, we find first the expressions in terms of the commutators and then calculate the respective commutators, obtaining the following expressions:

$$[S,H_{ep}] = [S,\sum_{i,\alpha} g_{i,\alpha}n_i({b_\alpha}^\dagger + b_\alpha)] \tag{26}$$

$$[S,H_{ep}] = \sum_{i,\alpha}\sum_{j,\beta}\frac{g_{i,\alpha}g_{j,\beta}}{\omega_\alpha}[n_j({b_\beta}^\dagger - b_\beta), n_i({b_\alpha}^\dagger + b_\alpha)] \tag{27}$$

which leads to:

$$[S,H_{ep}] = -2\sum_{i,j,\alpha}\frac{g_{i,\alpha}g_{j,\alpha}}{\omega_\alpha}n_in_j \tag{28}$$

Finally, it can be shown that for the electron-phonon interaction, the second order in the expansion just cancels out

$$[S,[S,H_{ep}]]=0 \tag{29}$$

and the resulting electron-phonon interaction term after the transformation reads:

$$(H_{ep})'=\sum_{i,\alpha} g_{i,\alpha} n_i ({b_\alpha}^\dagger + b_\alpha) - 2\sum_{i,j,\alpha}(g_{i,\alpha})(g_{i,\beta}) n_i n_j \tag{30}$$

Now, collecting all the terms we have calculated before we arrive to the following expression for the effective (*transformed*) Hamiltonian H':

$$\begin{aligned} H' = & -t\sum_i (c_i^\dagger c_{i+1} + c_{i+1}^\dagger c_i) - t\sum_{i,\alpha}\frac{g_{i,\alpha}}{\omega_\alpha}((b_\alpha)^\dagger - b_\alpha)(c_i^\dagger c_{i+1} + c_{i+1}^\dagger c_i) \\ & - t\sum_{i,\alpha,\beta}\frac{(g_{i,\alpha})}{\omega_\alpha}\frac{(g_{i,\beta})}{\omega_\beta}(c_i^\dagger c_{i+1} + c_{i+1}^\dagger c_i) + \sum_\alpha \omega_\alpha b_\alpha^\dagger b_\alpha - \sum_{i,\alpha} g_{i,\alpha} n_i (b_\alpha^\dagger + b_\alpha) \\ & + \sum_{i,j,\alpha}\frac{g_{i,\alpha}g_{j,\alpha}}{\omega_\alpha} n_i n_j + \sum_{i,\alpha} g_{i,\alpha} n_i ({b_\alpha}^\dagger + b_\alpha) - 2\sum_{i,j,\alpha}\frac{g_{i,\alpha}g_{i,\beta}}{\omega_\alpha} n_i n_j \end{aligned} \tag{31}$$

As it can be easily seen, some terms cancel out, and the final expression for transformed Hamiltonian becomes:

$$\begin{aligned} H' = & -t\sum_i \Bigg[(c_i^\dagger c_{i+1} + c_{i+1}^\dagger c_i) + -\sum_\alpha \frac{g_{i,\alpha}}{\omega_\alpha}((b_\alpha)^\dagger - b_\alpha)(c_i^\dagger c_{i+1} + c_{i+1}^\dagger c_i) - \\ & - \sum_{\alpha,\beta}\frac{g_{i,\alpha}}{\omega_\alpha}\frac{g_{i,\beta}}{\omega_\beta}(c_i^\dagger c_{i+1} + c_{i+1}^\dagger c_i)\Bigg] + \sum_\alpha \omega_\alpha b_\alpha^\dagger b_\alpha - \sum_{i,j,\alpha}\frac{g_{i,\alpha}g_{j,\alpha}}{\omega_\alpha} n_i n_j \end{aligned} \tag{32}$$

This new Hamiltonian H' has no direct electron-phonon interaction. The transformation results into a highly modified tunneling term, plus a last new term displaying an atractive electron-electron interaction whose strengh depends on the flexural modes of the carbon nanotube. So, we conclude that since Lang-Firsov is a unitary transformation, the effect of electron-photon interactions results in an attractive electron-electron interaction that helps to compensate for the Coulomb repulsion and stabilizes the system.

3 The quantum phase diagram of a single carbon nanotube hosting quantum dots

3.1 The phase diagram in the atomic limit (no tunneling)

After applying the Lang-Firsov transformation, the resulting Hamiltonian displayed in equation(32), still involves terms that are not diagonal. These terms correspond to the hopping of electrons from one quantum dot to another in the carbon nanotube, which under the Lang-Firsov transformation shifts the electron-phonon interactions to the tunneling. However, already a lot of insight can be gained if we take the atomic limit, $t=0$, in which no hopping occurs, and study the different possible configurations arising now the CNT. The corresponding Hamiltonian, H (we withdraw the notation H' for simplicity) is:

$$H(t=0) = \frac{U}{2}\sum_i n_i n_i + \sum_\alpha \omega_\alpha b_\alpha^\dagger b_\alpha - \sum_{i,j,\alpha} \frac{g_{i,\alpha} g_{j,\alpha}}{\omega_\alpha} n_i n_j \tag{33}$$

Moreover, since the bosonic energy term $\sum_\alpha \omega_\alpha b_\alpha^\dagger b_\alpha$ is constant, we withdraw it in the remainder of this work.

3.1.1 Case 1: Two electrons in a single carbon nanotube hosting two quantum dots

I start by considering the simplest possible scenario in which we have a single carbon nanotube with two quantum dots occupied by two unpolarized electrons. The Hilbert space is spanned by the 4 possible occupations of the two electrons in the two QD:$(\uparrow,\downarrow)$, $(\downarrow,\uparrow)$, $(\downarrow\uparrow,\_)$, and $(\_,\downarrow\uparrow)$. The Hamiltonian for this case is given by

$$H = \frac{U}{2}\sum_{i,\sigma\neq\sigma'} n_{i,\sigma} n_{i,\sigma'} - \sum_{i,j,m,\sigma,\sigma'} \frac{g_{i,m} g_{j,m}}{\omega_0} n_{i,\sigma} n_{j,\sigma'} \tag{34}$$

where we have replaced for easiness of reading the parameter α of the bosonic modes for m. Let us first calculate the value of the coupling constant. To this aim, we consider a classical model for the CNT (guitar modes). Writing the coupling constant in terms of the electrostatically tunable parameter g_0 one obtains:

$$g_{im} = g_0 \frac{2}{\pi}\frac{1}{\sqrt{m}}\int_{(i-1)\pi/2}^{(i)\pi/2} \sin(mx)dx = \frac{2g_0}{\pi}\frac{1}{m^{3/2}}\cos\left(m(i-1)\frac{\pi}{2} - \cos\frac{m\pi}{2}\right) \tag{35}$$

where we have performed a change of variables ($mdx = dt$) to perform the integral and used trigonometrical relations for the double angle to reach the above expression.

Now, we analyze the different configurations and their corresponding energies. We start with the Mott state, i.e., $(\uparrow,\downarrow)$ and the degenerate one $(\downarrow,\uparrow)$. In these cases, the on-site interaction term vanishes since the two electrons are never on the same site. Defining the parameter $\lambda = \frac{g^2}{\omega_0 U}$, it is trivial to see

$$\frac{E_{Mott}}{U} = -\lambda\frac{\pi^2}{3} \tag{36}$$

The second configuration in this system corresponds to the paired state also degenerate $(\downarrow\uparrow,\_)$, and $(\_,\downarrow\uparrow)$. The Hamiltonian now has an onsite Coulomb repulsion because now the two (unpolarized) electrons are on the same quantum dot and so the term doesn't vanish:

$$H = \frac{U}{2}\sum_i n_i n_i - \sum_m\sum_i \frac{(g_{im} n_i)^2}{m\omega_0} \tag{37}$$

We obtain:

$$\begin{aligned} E_{paired} &= 2U - \sum_{i,j,m} \frac{g_{i,m} g_{j,m}}{m\omega_0} n_i n_j \\ &= 2U - \frac{g_0^2}{\omega_0}\sin^2\left(\frac{m\pi}{4}\right)\left(\sin\left(\frac{m\pi}{4}\right) + \sin\left(\frac{3m\pi}{4}\right)\right)^2 \end{aligned} \tag{38}$$

To perform the sum over m, it should be noticed that only odds values of m give a contribution different from zero, and use that $\sum_m \sin^2 \frac{m\pi}{4} = (\frac{\sqrt{2}}{2})^2 = \frac{1}{2}$. We obtain: resulting into :

$$\frac{E_{paired}}{U} = 2 - \lambda \frac{\pi^2}{6} \tag{39}$$

Comparing the energy values for the two configurations: the Mott and the paired state, we observe that the Mott state will be the ground state until $E_{Mott} = E_{paired}$. A phase transition occurs for the critical value $\lambda_c = \frac{4}{\pi^2}$, where the paired state will become the ground state of the system. In the next step, we analyze the more complex case in which we have the CNT hosting four QD but with only two unpolarized electrons on it.

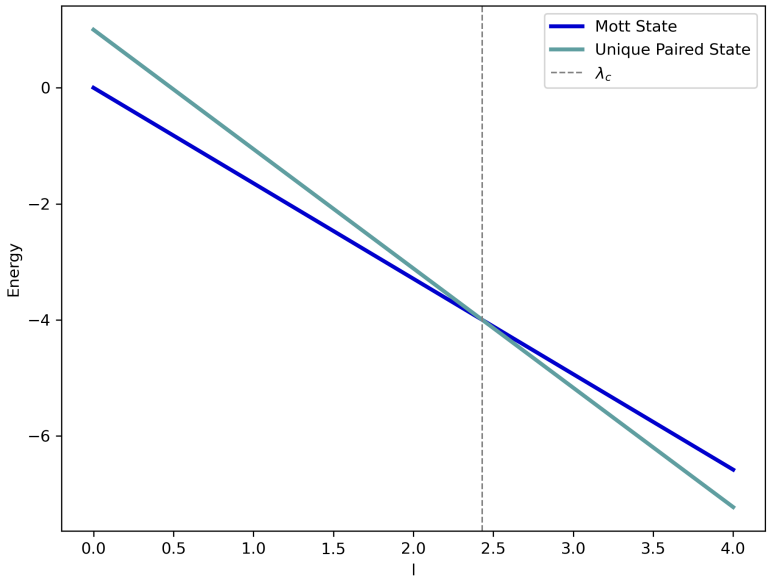

Figure 7: The plot displays the energy of ground state versus the parameter $\lambda = \frac{g^2}{\omega_0} U$ for a CNT with two QD on it. The QPT occurs at $\lambda_c = 2.43$ where the two states, Mott and the Paired state cross each other.

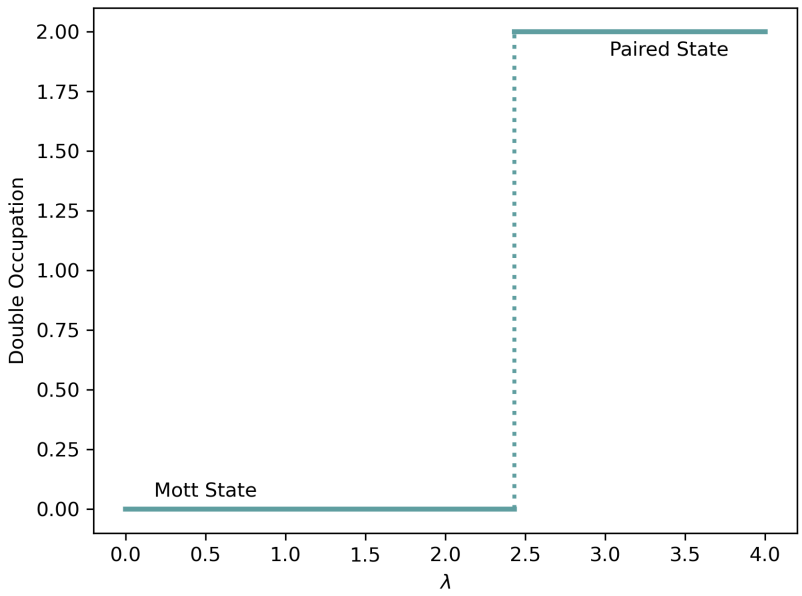

Figure 8: The QPT can be observed by looking at the electron occupany of the quantum dots versus λ also showing the sudden change at $\lambda_c = 2.43$ from the Mott state (with no double occupancy) into the new regime of Double Occupancy.

3.1.2 Case 2: Two electrons in a single carbon nanotube hosting four quantum dots

Here we increase the number of quantum dots to 4 while keeping the number of electrons at 2. Due to the greater number of dots our coupling constant changes to

$$g_{im} = g_0 \frac{8}{\pi} \frac{1}{m^{3/2}} \sin(\frac{m\pi}{8})(\sin[(2i-1)\frac{m\pi}{8}) \tag{40}$$

Mott States

First, we calculate the energies of the different electronic states. We begin by looking at the now wider class of Mott States, which we denote by Mott I- Mott IV.

Mott I $\quad \uparrow \quad \downarrow \quad \_\_ \quad \_\_$

As there is no double occupation present in a Mott State, the energy becomes

$$E_{M_I} = -\frac{g_0^2}{\omega_0} \sin^2\left(\frac{m\pi}{8}\right)\left(\sin\left(\frac{m\pi}{8}\right) + \sin\left(\frac{3m\pi}{8}\right)\right)^2 \tag{41}$$

By looking at the specific state, it becomes obvious that only terms with $i \in \{1,2\} \wedge j \in \{1,2\}$ contribute. Dividing by the on-site potential U, this gives:

$$\frac{E_{M_a}}{U} = -\frac{5}{24}\lambda\pi^2 \tag{42}$$

The configuration of the second Mott state is

Mott II $\quad \_\_ \quad \uparrow \quad \downarrow \quad \_\_$

The formula looks very similar to before with the slight difference that the electrons are moved to the center of the tube and so electron-phonon attractive energy changes:

$$E_{M_{II}} = -\frac{g_0^2}{\omega_0}\sin^2\left(\frac{m\pi}{8}\right)\left(\sin\left(\frac{3m\pi}{8}\right)+\sin\left(\frac{5m\pi}{8}\right)\right)^2 \tag{43}$$

resulting into

$$\frac{E_{M_{II}}}{U} = -\frac{1}{3}\lambda\pi^2 \tag{44}$$

We notice that the energy of this eigenstate M_b is lower in comparison with the previous configuration M_a. This configuration allows for the highest coupling between phonons and electrons taking all modes into account and, thereby, has the lowest energy of all the Mott States. The third Mott case corresponds to

Mott III $\underline{\uparrow}\quad\underline{\quad}\quad\underline{\downarrow}\quad\underline{\quad}$

now, the energy is

$$E_{M_{III}} = -\frac{g_0^2}{\omega_0}\sin^2\left(\frac{m\pi}{8}\right)\left(\sin\left(\frac{m\pi}{8}\right)+\sin\left(\frac{5m\pi}{8}\right)\right)^2 \tag{45}$$

which results into:

$$\frac{E_{M_{III}}}{U} = -\frac{17}{96}\lambda\pi^2. \tag{46}$$

The last Mott case corresponds to the following configuration

Mott IV $\underline{\uparrow}\quad\underline{\quad}\quad\underline{\quad}\quad\underline{\downarrow}$

whose energy reads:

$$E_{M_{IV}} = -\frac{g_0^2}{\omega_0}\sin^2\left(\frac{m\pi}{8}\right)\left(\sin\left(\frac{m\pi}{8}\right)+\sin\left(\frac{7m\pi}{8}\right)\right)^2 \tag{47}$$

resulting into:

$$\frac{E_{M_{IV}}}{U} = -\frac{1}{12}\lambda\pi^2 \tag{48}$$

Paired States

Next, we calculate the states of the Paired regime. Each state includes a term coming from the on-site potential. We also need to pay attention to the occupation operators ($n_i \in \{0,2\}\ \forall i$).

Paired I $\underline{\uparrow\downarrow}\quad\underline{\quad}\quad\underline{\quad}\quad\underline{\quad}$

$$E_{P_I} = \frac{U}{2}\sum_i n_{i,\sigma} n_{j,\sigma'} - \sum_{i,j,m} \frac{g_{i,m} g_{j,m}}{m\omega_0} n_i n_j \tag{49}$$

$$= U - 4\frac{g_0^2}{\omega_0}\sin^4\left(\frac{m\pi}{8}\right) \tag{50}$$

$$\frac{E_{P_I}}{U} = 1 - \frac{13}{96}\lambda\pi^2 \tag{51}$$

The second paired state is

Paired II 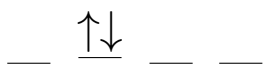

$$E_{P_{II}} = \frac{U}{2}\sum_i n_{i,\sigma} n_{j,\sigma'} - \sum_{i,j,m} \frac{g_{i,m} g_{j,m}}{m\omega_0} n_i n_j \tag{52}$$

$$= U - 4\frac{g_0^2}{\omega_0}\sin^2\left(\frac{m\pi}{8}\right)\sin^2\left(\frac{3m\pi}{8}\right) \tag{53}$$

$$\frac{E_{P_{II}}}{U} = 1 - \frac{37}{96}\pi^2\lambda \tag{54}$$

Quantum Phase Transition

To find if there is a Quantum Phase Transition we look for possible crossings between Mott states and Paired states and also at the occupation number. Our results are displayed in the next graphs, where a QPT occurs at $\lambda \approx 2$

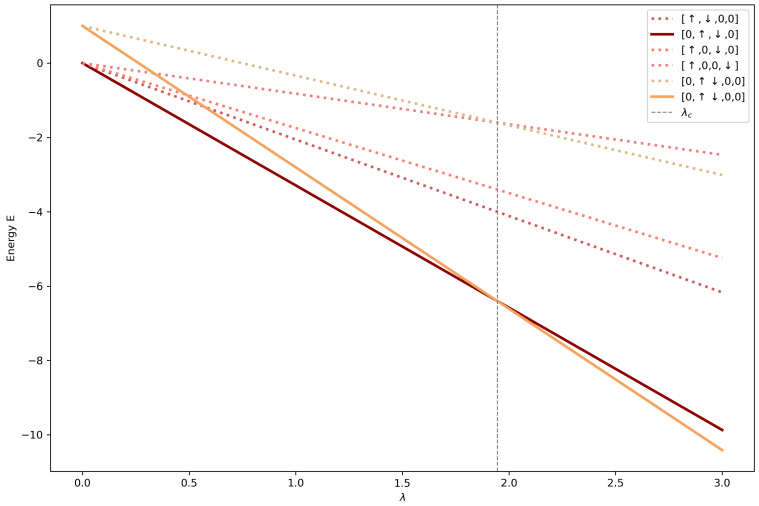

Figure 9: Energy of the two manifolds of (a) Mott States (different shades of red) and (b) the Paired states (brown) as a function of λ. The QPT occurs now at $\lambda_c = 1.95$ where the ground state suddenly changes its configuration from Mott to a Paired state.

The QPT indicates indeed a crossing between a Mott state and a Paired state. For $\lambda_c < \lambda$ the system evolves from single occupancy in a QD to double occupancy at $\lambda \geq \lambda_c$.

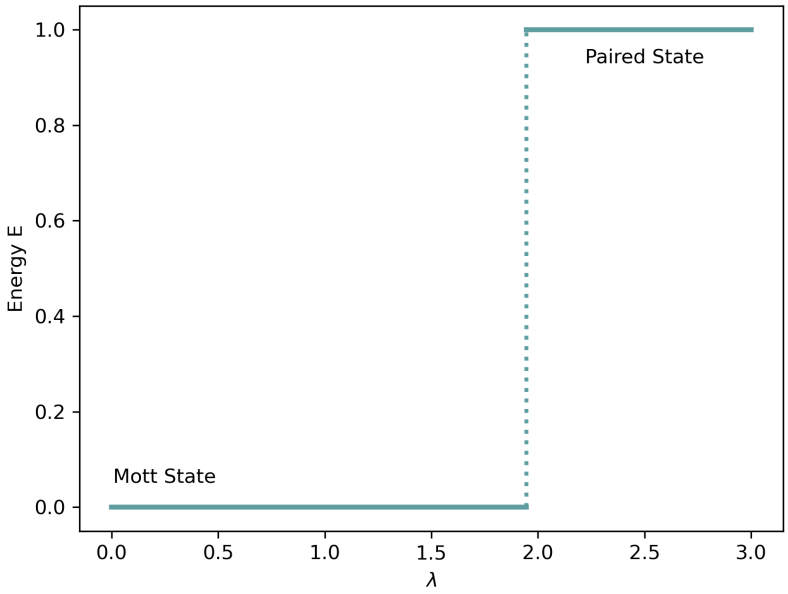

Figure 10: The quantum phase transition indicated from quantum dot occupancy shows how the ground state changes from a Mott to Paired at $\lambda_c = 1.95$

3.1.3 Case 3: Four electrons in a single carbon nanotube hosting four Quantum Dots

Here the setup is the one corresponding to the article [2], which for clarity we depicted it again below. As we will, see the number of possible quantum states in the CNT highly increases (from $n = 2^2$ to $n = 2^4$) as a result of increasing the number of electrons (each electron having two possible states up and down). Although now all Mott states are degenerated.

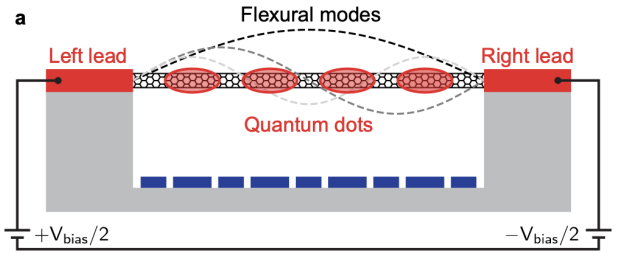

Figure 11: A suspended CNT within which four QD electrostatically formed on it. The dashed curves repreent the flexural modes of the CNT.

Mott States

In our chosen atomic limit, i.e., zero tunneling, all six Mott states are degenerate due to the electron-phonon interaction not being dependent on the spin.

Mott I $\uparrow \downarrow \uparrow \downarrow$

$$E = -\sum_{i,j,m} \frac{g_{i,m} g_{j,m}}{m\omega_0} n_i n_j \tag{55}$$

$$= -\frac{g_0^2}{\omega_0} \sum_{i,j,m} \frac{1}{m^4} \sin^2\left(\frac{m\pi}{8}\right) \sin\left(\frac{(2i-1)\pi}{8}\right) \sin\left(\frac{(2i-1)\pi}{8}\right) \tag{56}$$

$$\frac{E}{U} = 1 - \frac{2}{3}\pi^2 \lambda \tag{57}$$

Intermediate States

The first Intermediate we consider is:

Intermediate I $\uparrow \uparrow\downarrow \downarrow \_\_$

$$E = \frac{U}{2} \sum_i n_{i,\sigma} n_{j,\sigma'} - \sum_{i,j,m} \frac{g_{i,m} g_{j,m}}{m\omega_0} n_i n_j \tag{58}$$

$$\frac{E}{U} = 1 - \pi^2 \lambda \tag{59}$$

The second intermediate state:

Intermediate II 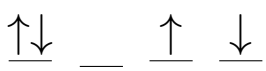

$$E = \frac{U}{2}\sum_i n_{i,\sigma} n_{j,\sigma'} - \sum_{i,j,m} \frac{g_{i,m} g_{j,m}}{m\omega_0} n_i n_j \tag{60}$$

$$\frac{E}{U} = 1 - \frac{15}{32}\pi^2 \lambda \tag{61}$$

Third one:

Intermediate III 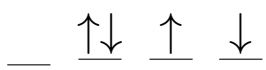

$$E = \frac{U}{2}\sum_i n_{i,\sigma} n_{j,\sigma'} - \sum_{i,j,m} \frac{g_{i,m} g_{j,m}}{m\omega_0} n_i n_j \tag{62}$$

$$\frac{E}{U} = 1 - \frac{31}{32}\pi^2 \lambda \tag{63}$$

Fourth,

Intermediate IV 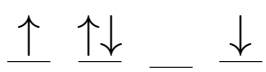

$$E = \frac{U}{2}\sum_i n_{i,\sigma} n_{j,\sigma'} - \sum_{i,j,m} \frac{g_{i,m} g_{j,m}}{m\omega_0} n_i n_j \tag{64}$$

$$\frac{E}{U} = 1 - \frac{23}{32}\pi^2 \lambda \tag{65}$$

Fifth

Intermediate V 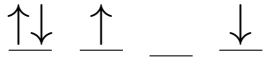

$$E = \frac{U}{2}\sum_i n_{i,\sigma} n_{j,\sigma'} - \sum_{i,j,m} \frac{g_{i,m} g_{j,m}}{m\omega_0} n_i n_j \tag{66}$$

$$\frac{E}{U} = 1 - \frac{1}{2}\pi^2 \lambda \tag{67}$$

The sixth one,

Intermediate VI 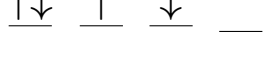

$$E = \frac{U}{2}\sum_i n_{i,\sigma} n_{j,\sigma'} - \sum_{i,j,m} \frac{g_{i,m} g_{j,m}}{m\omega_0} n_i n_j \tag{68}$$

$$\frac{E}{U} = 1 - \frac{23}{32}\pi^2 \lambda \tag{69}$$

Paired States

Now we look for the Paired states. First one:

Paired I $\underline{\uparrow\downarrow}$ $\underline{\uparrow\downarrow}$ $\underline{\quad}$ $\underline{\quad}$

with energy

$$E = \frac{U}{2}\sum_i n_{i,\sigma} n_{j,\sigma'} - \sum_{i,j,m} \frac{g_{i,m} g_{j,m}}{m\omega_0} n_i n_j \tag{70}$$

$$\frac{E}{U} = 2 - \frac{5}{6}\pi^2 \lambda \tag{71}$$

Second Paired state

Paired II $\underline{\uparrow\downarrow}$ $\underline{\quad}$ $\underline{\uparrow\downarrow}$ $\underline{\quad}$

$$E = \frac{U}{2}\sum_i n_{i,\sigma} n_{j,\sigma'} - \sum_{i,j,m} \frac{g_{i,m} g_{j,m}}{m\omega_0} n_i n_j \tag{72}$$

$$\frac{E}{U} = 2 - \frac{17}{24}\pi^2 \lambda \tag{73}$$

The third paired state

Paired III $\underline{\quad}$ $\underline{\uparrow\downarrow}$ $\underline{\uparrow\downarrow}$ $\underline{\quad}$

$$E = \frac{U}{2}\sum_i n_{i,\sigma} n_{j,\sigma'} - \sum_{i,j,m} \frac{g_{i,m} g_{j,m}}{m\omega_0} n_i n_j \tag{74}$$

$$\frac{E}{U} = 2 - \frac{4}{3}\pi^2 \lambda \tag{75}$$

and the last one:

Paired IV $\underline{\uparrow\downarrow}$ $\underline{\quad}$ $\underline{\quad}$ $\underline{\uparrow\downarrow}$

$$E = \frac{U}{2}\sum_i n_{i,\sigma} n_{j,\sigma'} - \sum_{i,j,m} \frac{g_{i,m} g_{j,m}}{m\omega_0} n_i n_j \tag{76}$$

$$\frac{E}{U} = 2 - \frac{1}{3}\pi^2 \lambda \tag{77}$$

Quantum Phase Transition

We present now the corresponding quantum phase transitions from a ground stata in the Mott configuration to a ground state in the Paired one.

Energy Plot

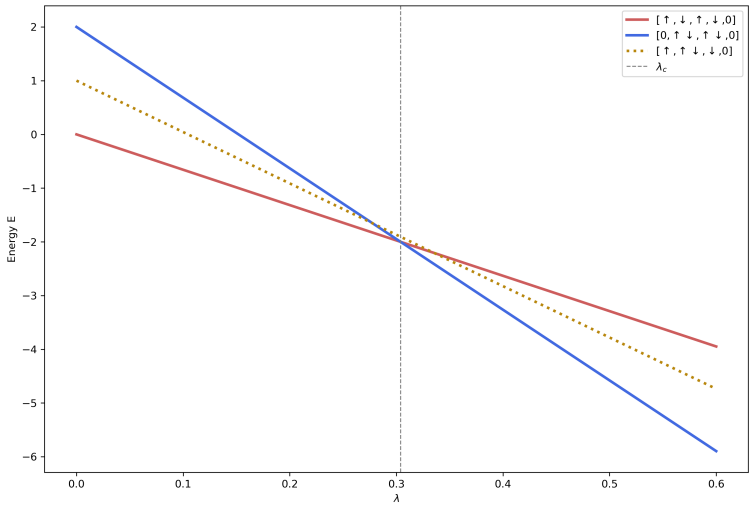

Figure 12: Energy of different electronic configurations versus the parameter λ (Here Mott, Intermediate and Paired State are indicated by red, brown, and blue colours respectively. The direct transition from Mott to Paired is easy to see as the lowest Intermediate is never the ground state. This transition occurs at $\lambda_c = 0.304$.

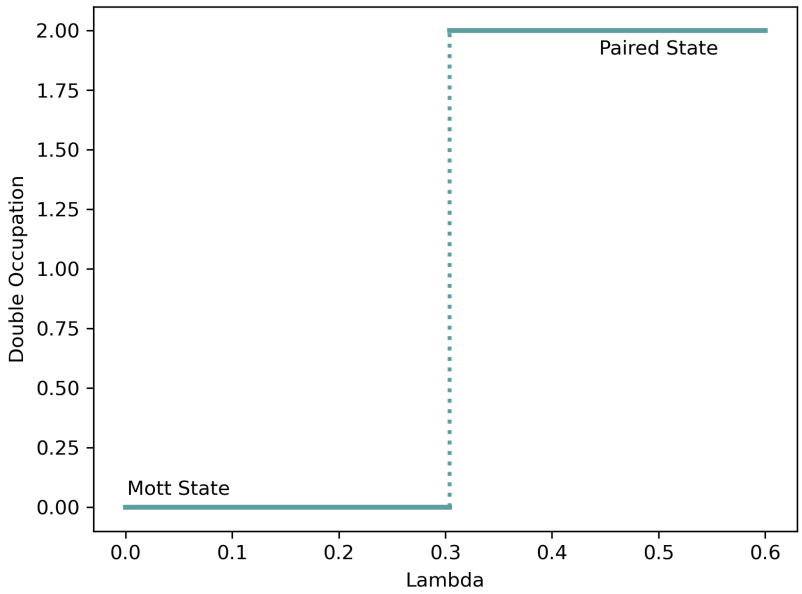

Figure 13: The quantum phase transition from Mott to Paired state can be easily identified by plotting the double occupancy versus the parameter λ, confirming that the QPT occurs at $\lambda_c = 0.304$. Our results are in line with the results of the previous works from ICFO.

3.2 The quantum phase diagram in the presence of tunneling: Perturbation Theory

To gain an insight into the effects that tunneling has on the quantum phase transitions of the system, one could assume that tunneling is sufficiently small and apply perturbation theory on the Lang-Firsov transformed Hamiltonian (32). To this aim, we use the obtained results for the eigenstates and eigenenergies from the Lang Firsov transformation, derived in the previous section. Furthermore, we will restrict our discussion to the phonon mode $m = 1$. From the previous discussion, we know that the system never chooses to be in an intermediate state which allows us to focus solely on the transition from Mott to Paired. We already know that for small λ the *Mott state* is preferred, while at higher values (equivalent to a greater coupling between electron and phonon) the *Unique paired state* forms the ground state. We are interested in how the introduction of tunneling may affect this transition. Due to Pauli's principle, we keep in the unpolarized spin setup, where pairing can belong to the ground state of the system. This implies that there are several manifolds of degenerate subspaces of states and forces us to *Degenerate Perturbation Theory*.

The eigenstates of the Hamiltonian obtained in the zero hopping limit that we will denote as $\hat{H}_0$ are split into manifolds of different eigenvalues. The hopping term, denoted by $\hat{H}_\mathrm{p}$, maps Mott and Paired states to the manifold of intermediate states. Consequently, a diagonalization of the Hamiltonian over only one of these subspaces is trivial. The solution to this issue is to introduce an effective Hamiltonian $\hat{H}_\mathrm{eff}$ which *does not* allow for tunneling in between manifolds of $\hat{H}_0$ but has the same eigenvalues as the original Hamiltonian $\hat{H} = \hat{H}_0 + t\hat{H}_\mathrm{p}$. This follows Cohen-Tannoudji *et al.* (1992).

The effective tunneling Hamiltonian is defined in the following way:

$$\hat{H}_{\text{eff}} = \hat{U}\hat{H}_t\hat{U}^\dagger. \tag{78}$$

with $\hat{U} := e^{i\hat{S}}$ and $\hat{S}$ Hermitian, $\hat{S} = \hat{S}^\dagger$ to ensure that $\hat{H}_{\text{eff}}$ is hermitian. However, as we have already seen, the tunneling term that results from applying the Lang-Firsov transformation is highly not trivial. To simplify the application of perturbation theory, we assume now that the only term that is relevant for perturbation theory after the transformation is the one corresponding to $H_{\text{eff}} = -t\sum_i(c_i c_i^\dagger + h.c.)$ defined via the original Hamiltonian as : Our chosen notation now is $|\alpha, i\rangle$ with α identifying the specific manifold and the index i the state within the degenerate subspace. In addition to imposing the degeneracy of the eigenvalues and allowing only transmissions within one manifold, we also impose the following on $\hat{S}$:

$$\hat{P}_\alpha\hat{S}\hat{P}_\alpha = 0 \text{ for any } \alpha. \tag{79}$$

P_α denotes a projector on to the subspace α. We once again use the Baker-Hausdorff formula:

$$\hat{H}_{\text{eff}} = \hat{H} + i[\hat{S}, \hat{H}] + \frac{1}{2!}i[\hat{S}, [\hat{S}, \hat{H}]] + \frac{1}{3!}i[\hat{S}, [\hat{S}, [\hat{S}, \hat{H}]]] + \frac{1}{3!}i[\hat{S}, [\hat{S}, \hat{S}\hat{H}]] + \cdots \tag{80}$$

Using a power-series Ansatz $\hat{S}$ with t as a parameter and applying the named requirements, we eventually end up with:

$$\langle\alpha, i|\hat{H}_{\text{eff}}|\alpha, j\rangle = E_{\alpha i}\delta_{ij} + t\langle\alpha, i|\hat{H}_{\text{int}}|\alpha, j\rangle - \langle\alpha, i|\hat{H}_{\text{p}}\hat{Q}_{\alpha i} + \hat{Q}_{\alpha j}\hat{H}_{\text{p}}|\alpha, j\rangle \tag{81}$$

with $\hat{Q}_{\alpha i} := \sum_{k,\gamma\neq\alpha}\frac{|\gamma,k\rangle\langle\gamma,k|}{E_{\gamma k}-E_{\alpha i}}$.

Coming back to our specific example: we choose the Mott State $[\uparrow,\downarrow,\uparrow,\downarrow]$ besides the uniquely Paired State. We will denote them with $|M\rangle$ and $|P\rangle$ from now on. Why we chose this specific Mott State will become more clear later. Letting $\hat{H}_{\text{p}}$ act on $|M\rangle$ results in a superposition of 12 intermediate states. These can be divided into 3 different blocks $\underline{\uparrow\downarrow}\ \underline{\ }\ \underline{\uparrow}\ \underline{\downarrow}$; $\underline{\ }\ \underline{\uparrow\downarrow}\ \underline{\uparrow}\ \underline{\downarrow}$; $\underline{\downarrow}\ \underline{\ }\ \underline{\uparrow\downarrow}\ \underline{\uparrow}$) with the following three eigenvalues respectively ($E_1 = 1 - \frac{15}{32}\pi^2\lambda$; $E_2 = 1 - \frac{31}{32}\pi^2\lambda$; $E_3 = 1 - \frac{23}{32}\pi^2\lambda$). For $\hat{H}_{\text{p}}$ acting on $|P\rangle$ we obtain a superposition of four states all of the second block.

Using equation 81 and our newly obtained knowledge of all possible transmissions we achieve the following correction term for the Mott State:

$$E^M_{\text{corr}} = E^M_0 - 2t^2\left(\frac{1}{E_1 - E_0} + \frac{1}{E_2 - E_0} + \frac{1}{E_3 - E_0}\right) \tag{82}$$

as well as the following expression for the Uniquely Paired State:

$$E^p_{\text{corr}} = E^p_0 - 4t^2\left(\frac{1}{E_2 - E_0}\right) \tag{83}$$

Keeping in mind that E^M_0 and E^P_0 are not the same values as before when had an infinite sum over all phonon modes. We have restricted ourselves to phonon mode m=1 which results in $E^M_0 = -\frac{64}{\pi^2}\lambda$ and $E^P_0 = 2 - \frac{128}{\pi^2}\lambda$. The results of our perturbation theory are displayed below. In Fig. 14, we choose the parameter $t/U = 0.025$, fulfilling that $t << U$. Despite our perturbation theory being very simple, and we have discarded a part of Lang-Firsov Hamiltonian that couples creation and annihilation operators with bosonic modes, we still notice the effects of hopping. In Fig, 15, we display the energy shift of the Mott state and the Paired state as a function of t/U, for a fixed value of λ, that is, for a fixed

value of the coupling constant between electrons and phonons g. Finally, in Fig. 16, one can observe how the presence of tunneling shifts the QPT to lower values of the parameter λ. Comparing this result with the numerical results obtained in [2], one sees that the shift is, nevertheless, incorrect. This is due to the fact that we have only considered a single term in the tunneling Hamiltonian equation 32, which is obviously not correct, and also due to the fact that we have restricted here to only the first mode $m = 1$ of the phononic bath. However, in this simplified model, the effect of degeneracies is visible and the QPT of the model changes significantly even for quite small values of the parameter t/U.

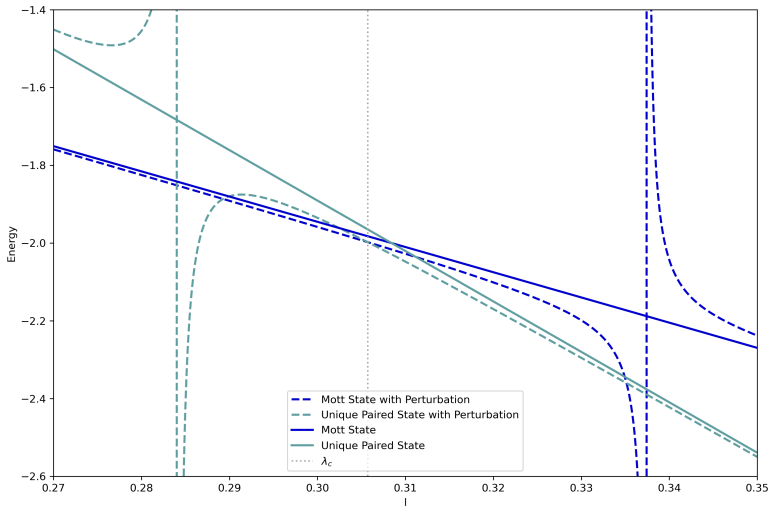

Figure 14: The Quantum Phase Transition occurs now at $\lambda_c = 0.307$ according to the simplified Perturbation Theory and for a value fixed value of tunneling $\frac{t}{U} = 0.025$.

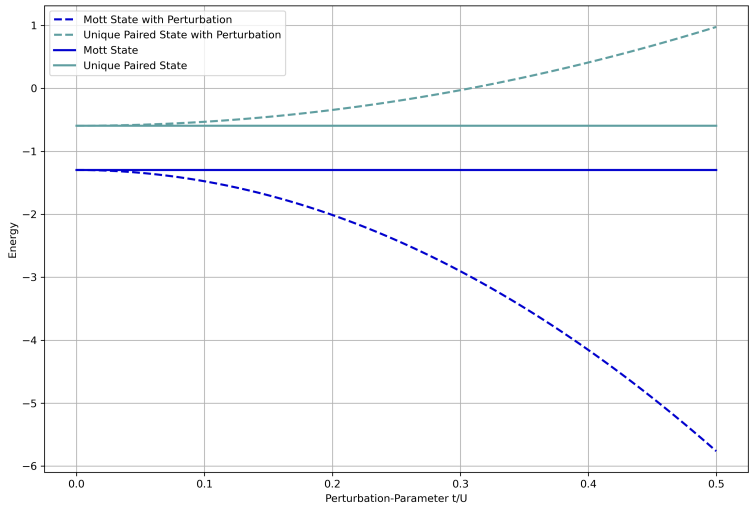

Figure 15: Energy shift of the Mott state and the Paired state as a function of the pertubation parameter t/U.

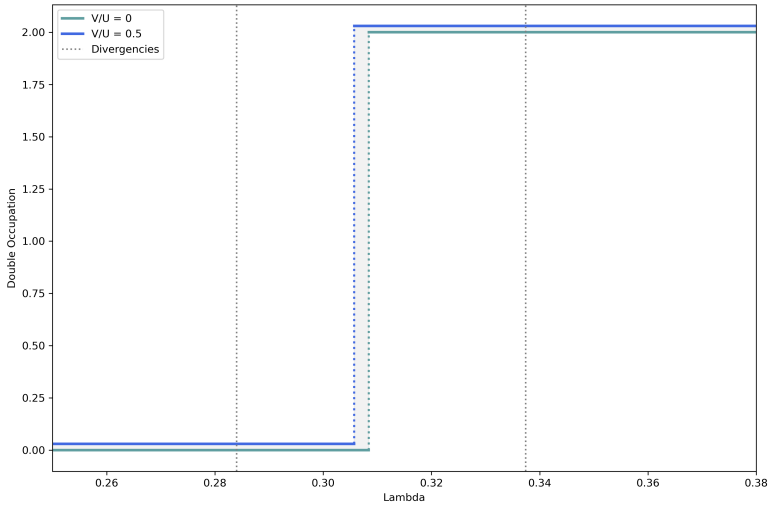

Figure 16: The plot of Double Occupation as function of λ with $\frac{t}{U} = 0.025$. The phase transition occurs at $\lambda_c = 0.307$

We finish this section by remarking that a proper perturbation theory should take into account all the terms proportional to the parameter t that appear as a result of the Lang-Firsov transformation in the original Hamiltonian. This is a rather complex and cumbersome task as the manifolds will have to include as well the modes of the CNT. Nevertheless, we have used a degenerate perturbation theory to observe a shift in the position of the QPT as a function of the tunneling parameter, as it should be expected. Even though the shift is not correct, one can obtain a proper shift by increasing "artificially" the weight of such term by a factor $\alpha = 4$, that is, using only the term $\alpha t \sum_i (c_i c_i^\dagger)$.

4 The quantum phase diagram of two coupled carbon nanotubes hosting quantum dots

In this section, we address the last part of this master thesis by proposing a new scheme in which two suspended nanotubes are sufficiently close to each other to allow Coulomb interactions between quantum dots. The richness of the model surpasses the goal of this master thesis, as we could also add tunneling between the adjacent quantum dots in different CNTs, as well as, analyzing the phase diagram when the two CNT have different vibration modes. This novel configuration is schematically presented in Figure (**??**.

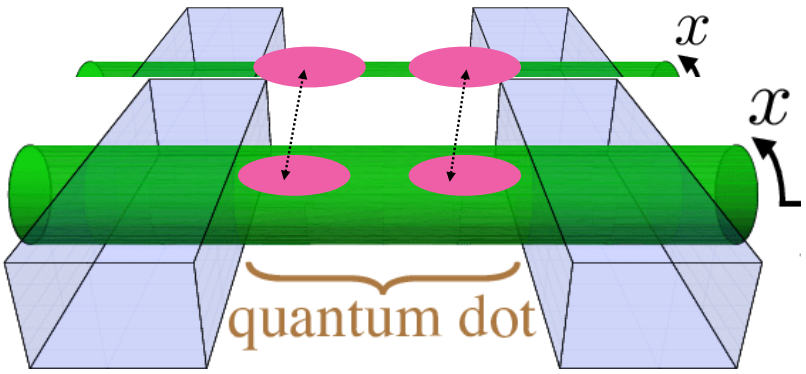

Figure 17: Schematically model of the setup consisting in two carbon nanotubes hosting different quantum dots and allowing the electrons on different CNT to interact (black arrows) via Coulomb interactions.

4.1 Two Interacting Nanotubes with four quantum dots and two electrons on each

Let us name the two CNTs as (A) and (B). Again, the simplest scenario and the only one we will consider here is the Hamiltonian in the atomic limit. Analytically, it is the only one which can still be addressed to obtain insight into full results. Extensions to more complex geometries and taking tunneling into account all variables (e.g. different phononic modes on each CNT, tunneling on each CNT independently, and inter-CNT tunneling), demands a not-at-all trivial numerical approach that we leave for future work.

The full Hamiltonian of the system now reads:

$$H_{AB} = H_A + H_B + H_{AB} \tag{84}$$

where

$$H^k = \frac{U}{2} \sum_{i,\sigma \neq \sigma'} n^k_{i,\sigma} n^k_{i,\sigma'} - \sum_{i,j,m,\sigma,\sigma'} \frac{g^k_{i,m} g^k_{j,m}}{\omega_0} n^k_{i,\sigma} n^k_{j,\sigma'} \tag{85}$$

with $k = A, B$. Interactions between the two CNTs is given by a Coulomb of the form

$$H_{AB} = V_{Coulomb} \sum_i n^A_i n^B_i \tag{86}$$

Thus, we only regard interaction between neighboring sites in different tubes and neglect Coulomb interactions between different sites in the same CNT and between different CNTs. In this setup, thus, we assume that the distance between the two CNTs is shorter than the distances between the QD on each CNT.

The addition of the second tube, as well as the now relevant Coulomb potential, increases our Hilbert space immensely. Especially the interaction between the tubes makes our tubes richer in the system we are considering. If we set the Coulomb potential to $V_{Coulomb} = 0$, the setup can be described by two isolated systems. Consequently, the observable physics is no different and the moment of phase transition should also occur at the same critical value that appeared for a single CNT hosting 4QD and 2 electrons, that

is at $\lambda_c = 1.95$. What should of course change, however, is the total energy of our system. The corresponding Hamiltonian is as follows:

$$H^{AB} = H^A + H^B + V_{Coulomb} \sum_i n_i n_i \tag{87}$$

$$= \frac{U^A}{2} \sum_i n^A_{i,\sigma} n^A_{j,\sigma'} - \sum_{i,j,m} \frac{g^A_{i,m} g^A_{j,m}}{m\omega^A_0} n^A_i n^A_j \tag{88}$$

$$+ \frac{U^B}{2} \sum_i n^B_{i,\sigma} n^B_{j,\sigma'} - \sum_{o,p,k} \frac{g^B_{o,k} g^B_{p,k}}{m\omega^B_0} n^B_i n^B_j + V \sum_i n^A_i n^B_i \tag{89}$$

For the discussion, let us introduce the following terminology: from now on, a Mott state means that systems A and B are in a Mott state; analogously, a paired state is when both systems are in a paired state. Intermediate state means that system A is in a Mott state and system B is in a paired state and vice versa. The Hilbert space can be divided into eight degenerate subspaces of type Mott; ten of type Intermediate, and five of type Paired. As before, the degeneracy is based on the arbitrary orientation in space, the independence of the attractive interaction from the orientation of the spin, and our assumption that the two tubes are aligned parallel to each other and thus the potential between the tubes is not dependent on the position of the quantum dots. Finally, we also concentrate only on the case where the relevant characteristics of the systems are identical, which further reduces the number of different intermediate states. The calculation of all energies of these subspaces would be tedious for the reader and we will therefore limit ourselves to the classes that are only relevant for the ground state.

Mott States: Mott I, Mott II and Mott III

Mott I

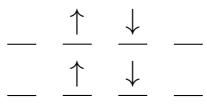

Mott II

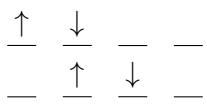

Mott III

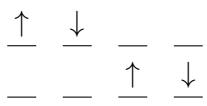

In the Mott regime, there are three different classes of states that compete for the role of the ground state. The first state corresponds to $\frac{V}{U} = 0$, both electrons are located on the inner quantum dots for both CNTs, as in Case II. As soon as the Coulomb potential has a value other than zero, the Mott state III shown is favored for lower λ values and transitions into Mott I at $\lambda_c = 0.405$. This means that our system is now subject to 2 quantum phase transitions. However, for large enough values of $\frac{V}{U}$, our system transitions directly from Mott state III to a paired state. The phase transition from Paired to Mott

is shifted to the left for an increasingly larger interaction potential. At the moment of the phase transition from Mott to Mott, all three Mott states (I, II, III) shown are degenerate.

Intermediate States

We describe now the Intermediate states appearing in the system

Intermediate I

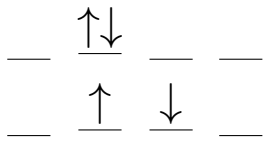

Intermediate II

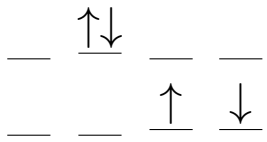

In the absence of coupling between the 2-CNT, that is, for $\frac{V}{U} = 0$, the state Intermediate I is degenerate at the quantum phase transition between Mott to Paired state, as indicated in Figure 18. However, for $\frac{V}{U} > 0$, the state Intermediate II is the one degenerate at quantum phase transition Mott-Mott or Mott-Paired for $\frac{V}{U} >> 1$.

Paired States

Paired I

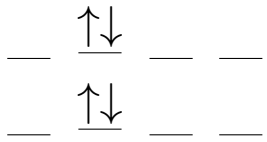

Paired II

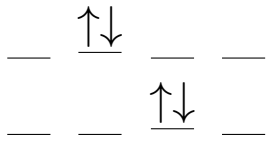

The energy for the lowest paired state is independent of the interaction between the tubes.

This is due to the number of electrons in this setup. With 2 electrons per tube, there are two states, which are initially degenerate and represent the lowest state of this type. While the energy of the first paired state is shifted upwards by the introduction of the Coulomb potential, the second is not affected, as indicated in the next Figures.

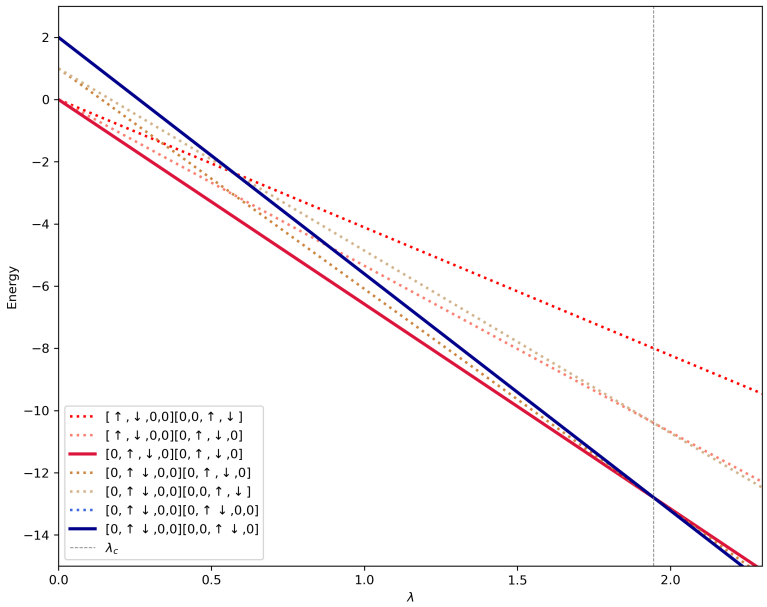

Figure 18: This is a plot of Energies at $\frac{V}{U} = 0$ showing Phase transition from Mott I to Paired II at $\lambda = 1.945$.

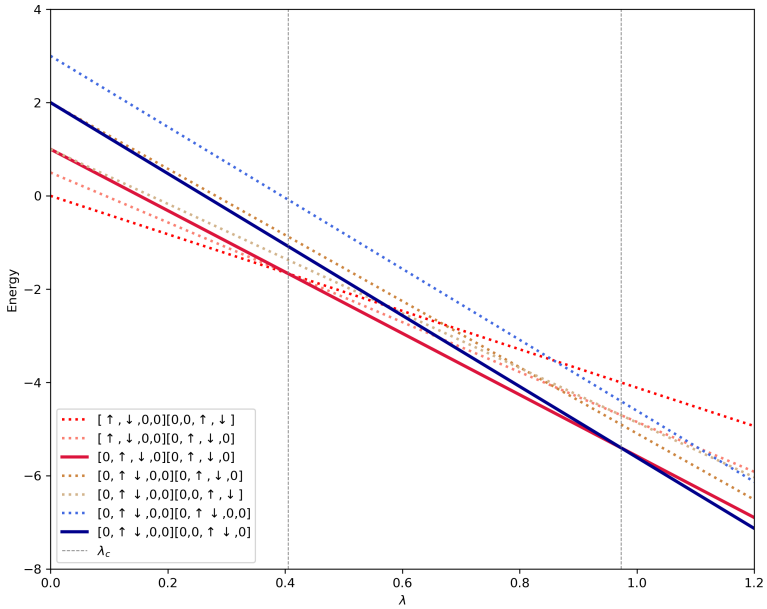

Figure 19: This Plot of Energies at $\frac{V}{U} = 0.5$ shows the two Phase transitions; from Mott III to Mott I at $\lambda = 0.405$ and Mott I then, into Paired II at $\lambda = 0.973$.

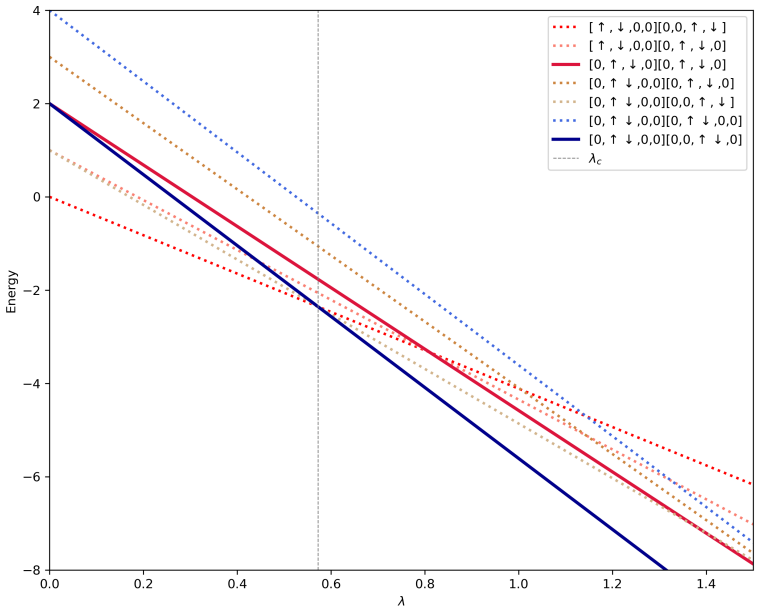

Figure 20: The Plot of Energies at $\frac{V}{U} = 1$ shows Phase transition from Mott III to Paired II at $\lambda = 0.572$ with a degenerate intermediate state II.

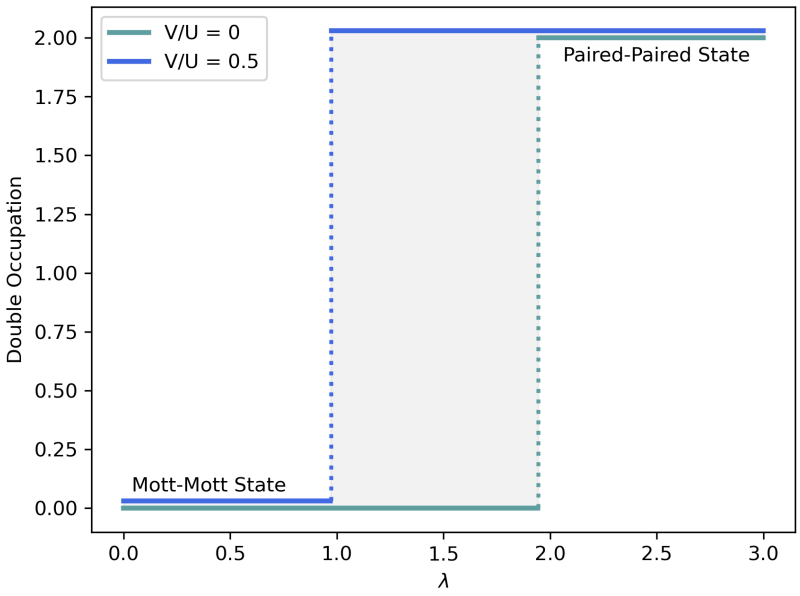

Figure 21: This plot shows Double occupancy as a function of λ for $\frac{V}{U} = 0$ and $\frac{V}{U} = 0.5$ with the Phase transitions occuring at $\lambda_c = 1.95$ and $\lambda_c = 0.973$.

5 Conclusions and further work

In this Master's thesis, we studied analytically a quantum simulator of the Electron-Phonon Class of Models through a system comprised of suspended Carbon Nanotube Quantum Dots. First, we derived the Hamiltonian of the system and applied the Lang-Firsov approximation to reduce the complexity of the electron-phonon interactions. Then, we study the quantum phase transition of the model in the atomic limit, that is, for tunneling equal to zero, In this limit, the study can be analytically carried on. We analyze different configurations from very simple ones to more complex ones. Further to account for tunneling effects, we used an oversimplified Degenerate Perturbation Theory. In the atomic limit, we considered first two quantum dots, sustained in one Carbon nanotube where we found Mott states to be the ground state until a critical point $\lambda_c = \frac{4}{(\pi)^2}$ at which there is a Phase transition into a regime where the Paired state is the ground state. Similarly, in the case of four quantum dots with two electrons, the Mott state is the ground state until $\lambda_c \approx 2$ after which the Paired states are the ground state. Then we proceeded to consider the case reported in [2], for 4 quantum dots with 4 electrons in a suspended carbon nanotube, reproducing the results they obtained.
Then, we used the Degenerate Perturbation theory to reproduce the results of the paper with the hopping taken into account. However, we made many oversimplifying assumptions that still showed us the effect of hopping on the QPT transitions, but due to these simplifications, we could not reproduce the results stated in [2]. Lastly, we extended this study to a new, and richer system which is now comprised of two carbon nanotubes where we assumed that the distance between the two CNTs is shorter than the inter-dot distance, implying that electrons hopping is favorable on different CNTs than within one. In this case, we found that for $\frac{V}{U} \neq 0$ the system now undergoes two phase transitions from Mott III to Mott I state and eventually from Mott to a Paired state as the value of λ increases.
As a recommendation for future work in this study, one could extend to the full Perturbation theory, continuing from what was done in this master's thesis, by taking into account all the hopping terms. The numerical solution of this problem which allows for the flexural modes to be more than $m = 1$ is also an interesting approach to solving the problem out of the atomic limit.
Furthermore, one can relax the assumptions we considered in this master's thesis by allowing CNTQD to be an open system such that it allows particle (electrons) flow between the first and last QD also allowing then μ to vary in the system and hence changing the Hamiltonian that was considered in this master's thesis. Added to this, one can also carry out an in-depth study of the application of two suspended CNTQD as quantum gates for application in quantum computing.

Bibliography

[1] AS Alexandrov and PE Kornilovitch. The fröhlich-coulomb model of high-temperature superconductivity and charge segregation in the cuprates. Journal of Physics: Condensed Matter, 14(21):5337, 2002.

[2] Utso Bhattacharya, Tobias Grass, Adrian Bachtold, Maciej Lewenstein, and Fabio Pistolesi. Phonon-induced pairing in quantum dot quantum simulator. Nano Letters, 21(22):9661–9667, 2021.

[3] I. G. Lang and Yu. A. Firsov. Kinetic theory of semiconductors with low mobility. Soviet Journal of Experimental and Theoretical Physics, 16:1301–1312, 1963.

[4] M. Lewenstein, A. Sanpera, and V. Ahufinger. Ultracold Atoms in Optical Lattices: Simulating quantum many-body systems. OUP Oxford, 2012.

[5] R. Tormo-Queralt, C. B. Møller, D. A. Czaplewski, G. Gruber, M. Cagetti, S. Forstner, N. Urgell-Ollé, J. A. Sanchez-Naranjo, C. Samanta, C. S. Miller, and A. Bachtold. Novel nanotube multiquantum dot devices. Nano Letters, 22(21):8541–8549, 2022. PMID: 36287197.

[6] Florian Vigneau, Juliette Monsel, Jorge Tabanera, Kushagra Aggarwal, Léa Bresque, Federico Fedele, Federico Cerisola, GAD Briggs, Janet Anders, Juan MR Parrondo, et al. Ultrastrong coupling between electron tunneling and mechanical motion. Physical Review Research, 4(4):043168, 2022.

[7] Lin Zhang, Utso Bhattacharya, Adrian Bachtold, Stefan Forstner, Maciej Lewenstein, Fabio Pistolesi, and Tobias Grass. Steady-state peierls transition in nanotube quantum simulator. npj Quantum Information, 9(1), January 2023.